Organometallics **1989**, *8*, 2107–2113

Synthesis and Characterization of Binuclear Zirconocene Complexes Linked by a Bridged Bis(cyclopentadienyl) Ligand

Karuna P. Reddy and Jeffrey L. Petersen*

Department of Chemistry, West Virginia University, Morgantown, West Virginia 26506-6045

Received November 7, 1988

The metathesis of $Li_2[X(C_5H_4)_2]$ with 2 equiv of $(C_5H_5)ZrCl_3\cdot 2THF$ or $(C_5Me_5)ZrCl_3$ offers a convenient method for the preparation of several binuclear zirconocenophane complexes $[X(C_5H_4)_2][(C_5R_5)ZrCl_2]_2$, where X = CH_2 or $SiMe_2$ and R = H or Me. Hydrolysis of $[X(C_5H_4)_2][(C_5H_5)ZrCl_2]_2$ in the presence of aniline affords the corresponding oxo-bridged derivatives $[X(C_5H_4)_2][(C_5H_5)ZrCl]_2(\mu\text{-}O)$. These compounds have been characterized by ^1H and ^{13}C NMR measurements and elemental analyses. The molecular structures of $[SiMe_2(C_5H_4)_2][(C_5Me_5)ZrCl_2]_2$ and $[SiMe_2(C_5H_4)_2][(C_5H_5)ZrCl]_2(\mu\text{-}O)$ were determined by X-ray diffraction methods and provided the opportunity to evaluate the structural response of the $[SiMe_2(C_5H_4)_2]^{2-}$ ligand to changes in the coordination environment of the two Zr centers. $[SiMe_2(C_5H_4)_2][(C_5Me_5)ZrCl_2]_2\cdot{}^1/_2C_7H_8$ crystallizes in a triclinic unit cell of $P\bar{1}$ symmetry with a = 9.219 (2) Å, b = 13.029 (3) Å, c = 15.928 (4) Å, α = 83.00 (2)°, β = 76.17 (2)°, γ = 78.58 (2)°, V = 1815.4 (8) Å^3, Z = 2, and d_{calcd} = 1.513 g/cm^3, whereas $[SiMe_2(C_5H_4)_2][(C_5H_5)ZrCl]_2(\mu\text{-}O)$ crystallizes in a monoclinic crystal lattice of $P2_1/c$ symmetry with a = 18.448 (4) Å, b = 9.665 (3) Å, c = 13.101 (3) Å, β = 100.95 (2)°, V = 2293 (1) Å^3, Z = 4, and d_{calcd} = 1.697 g/cm^3. Full-matrix least-squares refinements (based on F_o^2) of diffractometry data converged with final discrepancy indices of $R(F_o)$ = 0.037 with σ_1 = 1.72 and $R(F_o)$ = 0.029 with σ_1 = 1.10, respectively.

Introduction

Binuclear transition-metal complexes in which two reactive metal centers are held in close proximity offer the opportunity for observing cooperative chemical behavior.[1] Reactivity studies generally are aimed at evaluating how the mutual participation of both metal centers can enhance or modify the reactivity patterns normally exhibited by the corresponding mononuclear molecular fragments. The fundamental information gained from investigations of the influence of various stereochemical and electronic factors on the reactivity of these systems should ultimately contribute to the development of binuclear reagents that provide alternative routes for the sequential activation of various small molecular substrates.

Homo- and heterodinuclear transition-metal complexes which are resistant to fragmentation are particularly attractive for these studies. A common synthetic strategy involves the use of difunctional ligands, which are capable of coordinating to two different metal centers. For example, Casey,[2] Schore,[3] and others[4-6] have utilized modified cyclopentadienyl ligands, such as $[C_5H_4\text{–}P(C_6H_5)_2]^-$ and $[C_5H_4\text{–}SiMe_2CH_2PR_2]^-$, to construct heterobimetallic complexes in which the cyclopentadienyl ring is bonded to the electron-deficient early-transition-metal and the phosphine donor is coordinated to the electron-rich late-transition-metal center. Wolczanski and co-workers[7] have employed the alkoxyalkylphosphine ligand $[OCH_2PPh_2]^-$ as an alternative bridge for linking early- and late-transition-metal centers. However, in the case of homodinuclear complexes containing two high-valent metal centers, a difunctional ligand capable of stabilizing high metal oxidation states is needed. Two plausible candidates for this purpose are the fulvalene ligand, $C_{10}H_8^{2-}$, and the bridged bis(cyclopentadienyl) ligand, $[X(C_5H_4)_2]^{2-}$. Although binuclear fulvalene complexes containing either high-valent early[8] or low-valent late[9] transition metals are known, the fulvalene ligand can only accommodate a rather narrow range of metal···metal separations (2.8–3.6 Å). In contrast, the bridged bis(cyclopentadienyl) ligand offers the distinct advantage of being able to adjust the metal–

---

[1] For several recent examples of dinuclear activation in organometallic chemistry, see: (a) Lee, C.-L.; Hunt, C. T.; Balch, A. L. *Inorg. Chem.* **1981**, *20*, 2498. (b) Kubiak, C. P.; Woodcock, C.; Eisenberg, R. *Inorg. Chem.* **1982**, *21*, 2119. (c) Belmonte, P. A.; Cloke, F. G. N.; Schrock, R. R. *J. Am. Chem. Soc.* **1983**, *105*, 2643. (d) Schore, N. E.; Ilenda, C. S.; White, M. A.; Bryndza, H.; Matturo, M. G.; Bergman, R. G. *J. Am. Chem. Soc.* **1984**, *106*, 7451 and references cited therein. (e) Chisholm, M. H.; Hoffman, D. M.; Huffmann, J. C. *J. Am. Chem. Soc.* **1984**, *106*, 6806. (f) Sutherland, B. R.; Cowie, M. *Organometallics* **1985**, *4*, 1801. (g) Schenk, T. G.; Milne, C. R. C.; Sawyer, J. F.; Bosnich, B. *Inorg. Chem.* **1985**, *24*, 2338. (h) Arif, A. M.; Chandler, D. J.; Jones, R. A. *Organometallics* **1987**, *6*, 506. (i) Wu, J.; Fanwick, P. E.; Kubiak, C. P. *Organometallics* **1987**, *6*, 1805. (j) Ting, C.; Messerle, L. *J. Am. Chem. Soc.* **1987**, *109*, 6506.

[2] (a) Casey, C. P.; Bullock, R. M.; Fultz, W. C.; Rheingold, A. L. *Organometallics* **1982**, *1*, 1591. (b) Casey, C. P.; Nief, F. *Organometallics* **1985**, *4*, 1218. (c) Casey, C. P.; Bullock, R. M. *Acc. Chem. Res.* **1987**, *20*, 167.

[3] (a) Schore, N. E. *J. Am. Chem. Soc.* **1979**, *101*, 7410. (b) Schore, N. E.; Benner, L. S.; LaBelle, B. E. *Inorg. Chem.* **1981**, *20*, 3200.

[4] LeBlanc, J. C.; Moise, C.; Maisonnat, A.; Poilblanc, R.; Charrier, C.; Mathey, F. *J. Organomet. Chem.* **1982**, *231*, C43.

[5] Rausch, M. D.; Edwards, B. H.; Rogers, R. D.; Atwood, J. L. *J. Am. Chem. Soc.* **1983**, *105*, 3882.

[6] Tikkanen, W.; Fujita, Y.; Petersen, J. L. *Organometallics* **1986**, *5*, 888.

[7] (a) Ferguson, G. S.; Wolczanski, P. T. *Organometallics* **1985**, *4*, 1601. (b) Ferguson, G. S.; Wolczanski, P. T. *J. Am. Chem. Soc.* **1986**, 8293. (c) Ferguson, G. S.; Wolczanski, P. T.; Parkanyi, L.; Zonnevylle, M. C. *Organometallics* **1988**, 1967.

[8] (a) Guggenberger, L. J.; Tebbe, F. N. *J. Am. Chem. Soc.* **1973**, *95*, 7870. (b) Olthof, G. J. *J. Organomet. Chem.* **1977**, *128*, 367. Guggenberger, L. J.; Tebbe, F. N. *J. Am. Chem. Soc.* **1976**, *98*, 4137. (d) Lemenovskii, D. A.; Fedin, V. P.; Yanovskii, A.; Slovokhotov, V. L.; Struchkov, Y. T. *Koord. Khim.* **1980**, *6*, 882. (e) Perevalova, E. G.; Urazovskii, I. F.; Lemenovskii, D. A.; Slovokhotov, Y. L.; Struchkov, Y. T. *J. Organomet. Chem.* **1985**, *289*, 319. (f) Lemonovskii, D. A.; Fedin, V. P.; Slovokhotov, Y. L. *J. Organomet. Chem.* **1982**, *228*, 153. (g) Prout, K.; Caldwell, M. C. *Acta Crystallogr., Sect. B: Struct. Crystallogr. Cryst. Chem.* **1977**, *B33*, 2146. (h) Cooper, N. J.; Green, M. L. H.; Couldwell, C.; Prout, K. *J. Chem. Soc., Chem. Commun.* **1977**, 145. (i) Green, M. L. H.; Poveda, M. L.; Bashkin, J.; Prout, K. *J. Chem. Soc., Chem. Commun.* **1982**, 30. (j) Davison, A.; Wreford, S. S. *J. Am. Chem. Soc.* **1974**, *96*, 3017. (k) Brintzinger, H. H.; Bercaw, J. E. *J. Am. Chem. Soc.* **1969**, *91*, 7301. (l) Smart, J. C.; Curtis, C. J. *Inorg. Chem.* **1978**, *17*, 3290. (m) Smart, J. C.; Curtis, C. J. *Inorg. Chem.* **1977**, *16*, 1788. (n) Frederich, M. F.; Day, V. W.; Smart, J. C.; Pinsky, B. L. *J. Am. Chem. Soc.* **1979**, *101*, 4371. (o) Egan, J. W., Jr.; Petersen, J. L. *Organometallics* **1986**, *5*, 906. (p) Gambarotta, S.; Chiang, M. Y. *Organometallics* **1987**, *6*, 897. (q) Ashworth, T. V.; Agreda, T. C.; Herdtweck, E.; Hermann, W. A. *Angew. Chem., Int. Ed. Engl.* **1986**, *25*, 289.

[9] (a) Vollhardt, K. P. C.; Weidman, T. W. *Organometallics* **1984**, *3*, 82. (b) Vollhardt, K. P. C.; Weidman, T. W. *J. Am. Chem. Soc.* **1983**, *105*, 1976 and references cited therein. (c) Freman, M. J.; Orpen, A. G.; Connelly, N. G.; Manners, I.; Raven, S. J. *J. Chem. Soc., Dalton Trans.* **1985**, 2283. (d) Lacoste, M.; Astruc, D.; Garland, M.-T.; Varret, F. *Organometallics* **1988**, *7*, 2253 and references cited therein.

0276-7333/89/2308-2107$01.50/0 © 1989 American Chemical Society

metal separation by simply varying the size/length of the bridging group, X.

The conventional synthetic strategy employed for the preparation of binuclear complexes containing a bridged $[X(C_5H_4)_2]^{2-}$ ligand involves the metathetical reaction of 2 equiv of an appropriate organometal halide with the corresponding dilithio salt (eq 1). Due primarily to the

$$2L_nMCl + Li_2[X(C_5H_4)_2] \rightarrow X[(C_5H_4)ML_n]_2 + 2LiCl \quad (1)$$

initial paucity of suitable early-transition-metal halide precursors, the majority of binuclear complexes previously prepared by this route[10] contained electron-rich metal carbonyl fragments.[10a-j] However, with the recent emergence of the chemistry of sterically less crowded group 4 metal complexes, convenient synthetic procedures have been developed by Erker and co-workers[11] for $(C_5H_5)ZrCl_3$ and by Bercaw and Wolczanski[12] for $(C_5Me_5)ZrCl_3$ in good yield.

With the availability of these two monocyclopentadienyl Zr(IV) trichloride compounds, we have undertaken an effort to prepare a series of binuclear zirconocenophane complexes $[X(C_5H_4)_2][(C_5R_5)ZrCl_2]_2$ (X = CH_2, $SiMe_2$; R = H, Me), which contain two mechanically linked zirconocene dichloride units, and $[X(C_5H_4)_2][(C_5H_5)ZrCl]_2(\mu\text{-}O)$, in which the intramolecular oxo bridge further links the two Zr(IV) centers. Specific details regarding the synthesis and characterization of these binuclear zirconocenophane complexes are described. From a comparison of the molecular structures of $[SiMe_2(C_5H_4)_2][(C_5Me_5)ZrCl_2]_2$ and $[SiMe_2(C_5H_4)_2][(C_5H_5)ZrCl]_2(\mu\text{-}O)$, it has been possible to examine the structural response of the $[SiMe_2(C_5H_4)_2]^{2-}$ ligand to changes in the metal-coordination environment.

Experimental Section

Reagents. Reagent grade solvents were purified by using standard methods and freshly distilled under N_2. Toluene, benzene, and tetrahydrofuran were refluxed over potassium benzophenone ketyl, and pentane was dried over Na/K alloy. Each solvent was stored in a flask containing $[(C_5H_5)_2Ti(\mu\text{-}Cl)_2]_2Zn$.[13] Chlorinated solvents such as CCl_4, $CHCl_3$, and CH_2Cl_2 were distilled over P_4O_{10}, and each was stored in a flask containing P_4O_{10}. $(C_5H_5)ZrCl_3{\cdot}2THF$,[11] $(C_5Me_5)ZrCl_3$,[12] and C_5Me_5H[14] were prepared by using literature procedures. Dicyclopentadiene (Eastman), $SiMe_2Cl_2$ (Aldrich), CH_2Br_2 (Aldrich), *n*-butyllithium (Aldrich), and zirconocene dichloride (Boulder Chemical or Aldrich) were used as purchased without further purification. The deuterated solvents $CDCl_3$ (Aldrich, 99.8%), CD_2Cl_2 (Aldrich, 99.6%), and C_6D_6 (Aldrich, 99.5%) were dried over activated molecular sieves prior to use.

General Considerations. All manipulations were performed under a purified N_2 or Ar atmosphere on double manifold vacuum lines and in a Vacuum Atmospheres drybox. Air- and moisture-sensitive compounds were synthesized by using either standard Schlenk techniques or pressure-equalizing swivel filter frits equipped with Teflon stopcocks. All glassware was flame-dried under vacuum or oven-dried prior to use. Elemental analyses were performed by Galbraith Laboratories, Inc., Knoxville, TN. ^1H and ^{13}C NMR spectra were recorded on a JEOL GX-270 NMR spectrometer operating in the FT mode at 270 (^1H) and 67.5 MHz (^{13}C). The residual proton resonance (δ 7.24, chloroform-d_1; 5.32, methylene-d_2 chloride; 7.15, benzene-d_6) and ^{13}C resonance (δ 77.0, chloroform-d_1; 53.8, methylene-d_2 chloride; 128.0, benzene-d_6) of the solvent were used as the internal standards for the determination of chemical shifts relative to TMS.

Preparation of Dilithio Salts $Li_2[X(C_5H_4)_2]$ (X = CH_2, $SiMe_2$). The general reaction sequence used to prepare $Li_2[X(C_5H_4)_2]$ (X = CH_2 or $SiMe_2$) is initiated by the metathesis of 1 equiv of CH_2Br_2 or $SiMe_2Cl_2$ with 2 equiv of NaC_5H_5, respectively. Whereas $CH_2(C_5H_5)_2$ is distilled prior to the final metallation step, the less volatile $SiMe_2(C_5H_5)_2$ is readily separated by pentane extraction. Since the distillation step significantly reduces the amount of $CH_2(C_5H_5)_2$ obtained, the final yield of $Li_2[CH_2(C_5H_4)_2]$ (calculated on the basis of CH_2Br_2) is typically below 15%. On the other hand, the synthetic procedure outlined below for $Li_2[SiMe_2(C_5H_4)_2]$ provides substantially higher yields of this dilithio salt.

Freshly prepared NaC_5H_5 (4.4 g, 0.05 mol) is placed into a 250-mL flask, attached with a solv-seal joint to a swivel filter-frit assembly. After addition of ca. 150 mL of THF, the solution is cooled to −60 °C and $SiMe_2Cl_2$ (3.23 g, 0.025 mL) is added dropwise using a syringe. The reaction is stirred for 1 h at room temperature, and the THF is removed under vacuo. After addition of ca. 150 mL of pentane, the solution containing $SiMe_2(C_5H_5)_2$ is separated by filtration into another 250-mL flask attached to the other side of the filter frit. Upon cooling the pentane solution to −78 °C, 32 mL of a 1.6 M hexane solution of *n*-butyllithium is added dropwise. The reaction mixture is then rapidly stirred overnight at room temperature. The white insoluble product is isolated, washed twice with 50 mL of pentane, and then dried under vacuum, giving 3.2 g of $Li_2[SiMe_2(C_5H_4)_2]$ (64% yield).

Synthetic Procedure for the Preparation of $[X(C_5H_4)_2][(C_5R_5)ZrCl_2]_2$ (X = CH_2, $SiMe_2$; R = H, Me). The same basic procedure was used to prepare each of these four binuclear zirconocenophane complexes by the metathetical reaction of $(C_5H_5)ZrCl_3{\cdot}2THF$ or $(C_5Me_5)ZrCl_3$ with $Li_2[X(C_5H_4)_2]$. Consequently, only the preparation of one of these compounds, namely, $[SiMe_2(C_5H_4)_2][(C_5Me_5)ZrCl_2]_2$, will be described.

Fresh-sublimed $(C_5Me_5)ZrCl_3$ (1.67 g, 5 mmol) and $Li_2[SiMe_2(C_5H_4)_2]$ (0.50 g, 2.5 mmol) were weighed into a 100-mL flask. Toluene was added, and the reaction mixture was refluxed overnight. After solvent removal CH_2Cl_2 was added and the resulting pale yellow solution was separated by filtration. The pale yellow product was washed with petroleum ether/benzene and recrystallized from toluene yielding 1.3 g of $[SiMe_2(C_5H_4)_2][(C_5Me_5)ZrCl_2]_2{\cdot}{}^1/_2C_7H_8$, (65% yield). The presence of toluene was confirmed by the appearance of appropriate proton resonances (δ 7.09, 7.00, 6.98, and 2.09) in the solution NMR spectrum ($CDCl_3$). The toluene can be removed by recrystallization from CH_2Cl_2 followed by washing with pentane.

Anal. Calcd for unsolvated $C_{32}H_{44}Zr_2Cl_4Si$: C, 49.20; H, 5.67. Found: C, 48.44; H, 5.45.

The corresponding yields obtained by using a comparable reaction scale and the analytical data for the remaining zirconocenophane complexes are given below:

For $[SiMe_2(C_5H_4)_2][(C_5H_5)ZrCl_2]_2$: 65% yield. Anal. Calcd for $C_{22}H_{24}Zr_2Cl_4Si$: C, 41.24; H, 3.78. Found: C, 41.30; H, 3.92.

For $[CH_2(C_5H_4)_2][(C_5Me_5)ZrCl_2]_2$: 89% yield. Anal. Calcd for $C_{31}H_{40}Zr_2Cl_4$: C, 50.53; H, 5.47. Found: C, 50.35; H, 5.54.

For $[CH_2(C_5H_4)_2][(C_5H_5)ZrCl_2]_2$: 48% yield. Anal. Calcd for $C_{21}H_{20}Zr_2Cl_4$: C, 42.27; H, 3.38. Found: C, 42.75; H, 3.52.

The ^1H and ^{13}C NMR data for these four zirconocenophane compounds are summarized in Table I.

Synthetic Procedure for the Preparation of $[X(C_5H_4)_2][(C_5H_5)ZrCl]_2(\mu\text{-}O)$ (X = CH_2, $SiMe_2$). The hydrolysis of $[X(C_5H_4)_2][(C_5H_5)ZrCl_2]_2$ (X = CH_2, $SiMe_2$) in the presence of aniline provides a convenient method[15] for preparing the

---

[10] (a) Weaver, J.; Woodward, P. *J. Chem. Soc., Dalton Trans.* **1973**, 1439. (b) Wegner, P. A.; Uski, V. A.; Kiester, R. P.; Dabestani, S.; Day, V. W. *J. Am. Chem. Soc.* **1977**, *99*, 4846. (c) Bergman, R. G. *Acc. Chem. Res.* **1980**, *13*, 113 and references cited therein. (d) Nelson, G. O.; Wright, M. E. *J. Organomet. Chem.* **1981**, *206*, C21. (e) Wright, M. E.; Mezza, T. M.; Nelson, G. O.; Armstrong, N. R.; Day, V. W.; Thompson, M. R. *Organometallics* **1983**, *2*, 1711. (f) Werner, H.; Scholz, H. J.; Zolk, R. *Chem. Ber.* **1985**, *118*, 4531. (g) Walter, A.; Heck, J. *J. Organomet. Chem.* **1986**, *302*, 363. (h) Scholtz, H. J.; Werner, H. *J. Organomet. Chem.* **1986**, *303*, C8. (i) Bitterwolf, T. E. *J. Organomet. Chem.* **1986**, *312*, 197. (j) Bitterwolf, T. E.; Rheingold, A. L. *Organometallics* **1987**, *6*, 2138. (k) Katz, T. J.; Acton, N.; Martin, G. *J. Am. Chem. Soc.* **1969**, *91*, 2804. (l) Cassens, A.; Eilbracht, P.; Nazzal, A.; Prossdorf, W.; Muller-Westerhoff, U. T. *J. Am. Chem. Soc.* **1981**, *103*, 6367. (m) Hock, N.; Oroschin, W.; Paolucci, G.; Fisher, R. D. *Angew. Chem., Int. Ed. Engl.* **1986**, *25*, 738.

[11] Erker, G.; Berg, K.; Treschanke, L.; Engel, K. *Inorg. Chem.* **1982**, *21*, 1277.

[12] Wolczanski, P. T.; Bercaw, J. E. *Organometallics* **1982**, *1*, 793.

[13] Sekutowski, D. G.; Stucky, G. D. *Inorg. Chem.* **1975**, *14*, 2192.

[14] Threlkel, R. S.; Bercaw, J. E. *J. Organomet. Chem.* **1977**, *136*, 1.

[15] Wailes, P. C.; Weigold, H. *J. Organomet. Chem.* **1970**, *24*, 405.

Table I. Summary of ^{1}H and ^{13}C NMR Data[a]

compd	solv	assignt	^{1}H NMR	^{13}C NMR
$[SiMe_2(C_5H_4)_2][(C_5Me_5)ZrCl_2]_2$	C_6H_6	C_5H_4	6.22 (t, 2.6)	128.2 (s)[b]
			5.90 (t, 2.6)	125.5 (dq, 173, 7)
				115.3 (dq, 171, 7)
		C_5Me_5		124.4 (s)
		$C_5\mathit{Me}_5$	1.78 (s)	12.8 (q, 127)
		$SiMe_2$	0.43 (s)	−0.60 (q, 121)
$[SiMe_2(C_5H_4)_2][(C_5H_5)ZrCl_2]_2$	$CDCl_3$	C_5H_4	6.60 (t, 2.5)	125.35 (dq, 174, 7.7)
			6.44 (t, 2.5)	124.64 (s)[b]
				117.25 (dq, 174, 7.7)
		C_5H_5	6.28 (s)	116.10 (dqt, 175, 6.6)
		$SiMe_2$	0.53 (s)	1.02 (q, 118)
$[CH_2(C_5H_4)_2][(C_5Me_5)ZrCl_2]_2$	C_6D_6	C_5H_4	5.98 (t, 2.7)	133.33 (s)[b]
			5.65 (t, 2.7)	116.90 (dm, 178)
				113.48 (dm, 172)
		C_5Me_5		124.01 (s)
		$C_5\mathit{Me}_5$	1.78 (s)	12.31 (q, 127)
		CH_2	4.27	31.01[c]
$[CH_2(C_5H_4)_2][(C_5H_5)ZrCl_2]_2$	CD_2Cl_2	C_5H_4	6.37 (t, 2.7)	132.78 (s)[b]
			6.23 (t, 2.7)	117.44 (dm, 170)
				113.60 (dm, 176)
		C_5H_5	6.45 (s)	116.33 (dm, 177)
		CH_2	3.98 (s)	31.01[c]
$[SiMe_2(C_5H_4)_2][(C_5H_5)ZrCl]_2(\mu\text{-}O)$	$CDCl_3$	C_5H_4	6.56 (m)	126.87 (m)[b]
			6.51 (m)	125.02 (dm, 170, 4.9)
			6.45 (m)	118.30 (dm, 175, 7.3)
			6.36 (m)	114.60 (dm, 163, 4.9)
				113.62 (dm, 168, 6.1)
		C_5H_5	6.29 (s)	114.20 (dqt, 173, 6.7)
		$SiMe_2$	0.42	−1.20 (q, 119)
$[CH_2(C_5H_4)_2][(C_5H_5)ZrCl]_2(\mu\text{-}O)$	C_6D_6 (^{1}H) CD_2Cl_2 (^{13}C)	C_5H_4	6.04 (m)	136.78 (s)[b]
			5.98 (m)	116.64 (dm, 167)
			5.52 (m)[d]	116.07 (dm, 180)
				110.10 (dm, 172)
				105.82 (dm, 168)
		C_5H_5	6.08 (s)	114.43 (dm, 176)
		CH_2	3.18 (s)	29.47[c]

[a] Chemical shifts are in ppm. $^3J_{H\text{-}H}$ and $^{1,2}J_{C\text{-}H}$ in Hz are given in parentheses. Notation for various proton coupling patterns: dq = doublet of quartets; dqt = doublet of quintets; dm = doublet of multiplets. [b] Resonance assigned to bridgehead carbon. [c] Limited solubility of this compound hindered efforts to observe the triplet for the bridging CH_2 group in the gated nondecoupled ^{13}C spectrum. [d] Overlapping pair of multiplets.

corresponding oxo-bridged derivatives $[X(C_5H_4)_2][(C_5H_5)ZrCl]_2(\mu\text{-}O)$. The synthesis of the dimethylsilyl-bridged compound proceeds as follows: To 75 mL of a CH_2Cl_2 solution containing 1.00 g (1.6 mmol) of $[SiMe_2(C_5H_4)_2][(C_5H_5)ZrCl_2]_2$ is added 0.29 g (3.2 mmol) of aniline and 0.03 mL (1.6 mmol) of H_2O with continuous stirring. The soluble oxo-bridged product is separated by filtration. After the volume of the filtrate is reduced to ca. 10 mL, pentane is added. The white finely divided product is isolated and air-dried. Recrystallization yielded 0.66 g (73% yield) of $[SiMe_2(C_5H_4)_2][(C_5H_5)ZrCl]_2(\mu\text{-}O)$.

Anal. Calcd for $C_{22}H_{24}Zr_2Cl_2SiO$: C, 45.10; H, 4.13. Found: C, 45.52; H, 4.32.

For $[CH_2(C_5H_4)_2][(C_5H_5)ZrCl]_2(\mu\text{-}O)\cdot C_6H_6$: 70% yield. Anal. Calcd for $C_{27}H_{26}Zr_2Cl_2O$: C, 52.31; H, 4.22. Found: C, 51.99; H, 4.15.

The ^{1}H and ^{13}C NMR data for these two oxo-bridged zirconocenophane compounds are listed in Table I.

X-ray Data Collection and Structural Analyses. X-ray diffraction methods were used to determine the solid-state structures of $[SiMe_2(C_5H_4)_2][(C_5Me_5)ZrCl_2]_2$ and the two oxo-bridged derivatives $[X(C_5H_4)_2][(C_5H_5)ZrCl]_2(\mu\text{-}O)$ (X = CH_2, $SiMe_2$). For purposes of brevity, only the structural analyses of the two dimethylsilyl-bridged compounds will be presented. All of the structural analyses were performed by using the same general procedures previously described elsewhere.[16]

In each case, a crystal was sealed in a glass-capillary tube under a prepurified N_2 atmosphere and then optically aligned on a Picker full-circle goniostat controlled by a Krisel Control diffractometer automation system. Low-angle reflections ($5° < 2\theta < 10°$) were used in conjunction with an autoindexing routine to estimate the lattice parameters. The orientation angles (ω, χ, 2θ) for 20 higher angle reflections were optimized by a peak-centering algorithm and then least-squares fit to give the corresponding refined lattice parameters in Table II.

Intensity data were measured with Zr-filtered Mo Kα X-ray radiation ($\lambda(K_{\alpha_1}) = 0.709\,26$ Å, $\lambda(K_{\alpha_2}) = 0.713\,54$ Å) at a takeoff angle of 2°. Each diffraction peak was scanned at a fixed rate (θ–2θ mode) with the scan width calculated from the expression $\omega = A + B \tan \theta$. Background counts were measured at the extremes of each scan with crystal and detector kept stationary. During data collection the intensities of three standard reflections were measured periodically. The integrated intensity, I, and its standard deviation, $\sigma_c(I)$, for each of the measured peaks were calculated from the expressions $I = w(S/t_s - B/t_b)$ and $\sigma_c(I) = w(S/t_s^2 + B/t_b^2)^{1/2}$, where S represents the total scan count measured in time t_s and B is the combined background count in time t_b. The intensity data were corrected for absorption[17] and Lorentz–polarization effects. The standard deviation of the square of each structure factor, $F_o^2 = AI/Lp$, was calculated from $\sigma(F_o^2) = [\sigma_c(F_o^2)^2 + (pF_o^2)^2]^{1/2}$, and equivalent reflections were averaged.

The initial coordinates of the two independent Zr atoms in $[SiMe_2(C_5H_4)_2][(C_5Me_5)ZrCl_2]_2$ and $[SiMe_2(C_5H_4)_2][(C_5H_5)ZrCl]_2(\mu\text{-}O)$ were estimated from an analysis of the interatomic vectors appearing on the corresponding unsharpened three-dimensional Patterson map. Subsequent Fourier summations provided approximate coordinates for the remaining non-hydrogen atoms. In the former case, a difference Fourier summation eventually revealed the presence of residual peaks in the vicinity

---

(16) Jones, S. B.; Petersen, J. L. *Inorg. Chem.* **1981**, *20*, 2889.

(17) The absorption correction was performed with the use of the general polyhedral shape routine of DTALIB. The distance from the crystal center to each face and the orientation angles (ϕ and χ) used to place each face in diffracting position are required to define the crystal's shape, size, and orientation with respect to the diffractometer's coordinated system.

Table II. Data for X-ray Diffraction Analyses of $[SiMe_2(C_5H_4)_2][(C_5Me_5)ZrCl_2]_2 \bullet {}^1/_2C_7H_8$ (I) and $[SiMe_2(C_5H_4)_2][(C_5H_5)ZrCl]_2(\mu\text{-}O)$ (II)

	I	II
	A. Crystal Data	
mol formula	$C_{35.5}H_{48}Zr_2Cl_4Si$	$C_{22}H_{24}Zr_2Cl_2SiO$
cryst system	triclinic	monoclinic
space group	$P\bar{1}$	$P2_1/c$
a, Å	9.219 (2)	18.448 (4)
b, Å	13.029 (3)	9.665 (3)
c, Å	15.928 (4)	13.101 (3)
α, deg	83.00 (2)	
β, deg	76.17 (2)	100.95 (2)
γ, deg	78.58 (2)	
V, Å^3	1815.4 (8)	2293 (1)
fw, amu	827.11	585.89
d(calcd), g/cm^3	1.513	1.697
Z	2	4
μ, cm^{-1}	9.1	11.83
	B. Data Collection and Analysis Summary	
cryst dimens, mm	0.40 × 0.30 × 0.20	0.45 × 0.475 × 0.125
reflctns sampled	$\pm h,\pm k,l$	$\pm h,k,l$
2θ range for centered reflctns, deg	$30 < 2\theta < 35$	$30 < 2\theta < 35$
scan rate, deg/min	2	2
scan width, deg	$1.1 + 0.7 \tan\theta$	$1.0 + 0.7 \tan\theta$
no. of std reflctns	3	3
% cryst decay	0	0
no. of unique data used	5148 ($F_o^2 > \sigma(F_o^2)$)	4058 ($F_o^2 > 0$)
agreement between equiv data		
$R_{av}(F_o)$	0.013	0.018
$R_{av}(F_o^2)$	0.020	0.014
transmissn coeff	0.80–0.85	0.65–0.87
p	0.03	0.03
discrepancy indices for data with $F_o^2 > \sigma(F_o^2)$		
$R(F_o)$	0.037	0.029
$R(F_o^2)$	0.054	0.032
$R_w(F_o^2)$	0.083	0.075
σ_1	1.72	1.10
no. of variables	484	349
data to parameter ratio	10.6:1	11.7:1

Table III. Selected Interatomic Distances (Å) and Bond Angles (deg) for the Non-Hydrogen Atoms in $[SiMe_2(C_5H_4)_2][(C_5Me_5)ZrCl_2]_2$[a–c]

A. Interatomic Distances			
Zr1–C11	2.465 (1)	Zr2–Cl3	2.448 (1)
Zr1–Cl2	2.436 (1)	Zr2–Cl4	2.444 (1)
Zr1···Cp*1	2.219 (4)	Zr2···Cp*2	2.225 (4)
Zr1···Cp1	2.229 (4)	Zr2···Cp2	2.225 (4)
Si–C11	1.873 (5)	Si–C16	1.879 (4)
Si–MC11	1.844 (7)	Si–MC12	1.871 (6)
Zr1–C(Cp*1 ring) range: 2.512 (4)–2.534 (5)			
Zr2–C(Cp*2 ring) range: 2.505 (4)–2.555 (4)			
Zr1–C(Cp1 ring) range: 2.485 (5)–2.564 (4)			
Zr2–C(Cp2 ring) range: 2.483 (4)–2.583 (4)			
C–C (Cp* rings) range: 1.406 (6)–1.419 (5)			
Cn–MC*n* (*n* = 1–10) range: 1.478 (8)–1.505 (9)			
C–C (Cp rings) range: 1.388 (8)–1.431 (6)			
B. Bond Angles			
Cl1–Zr1–Cl2	93.58 (4)	Cl3–Zr2—Cl4	98.20 (5)
Cp*1–Zr1–Cp1	132.0 (1)	Cp*2–Zr2–Cp2	129.5 (2)
C11–Si–MC11	113.1 (2)	C16–Si–MC11	114.0 (2)
C11–Si–MC12	110.8 (3)	C16–Si–MC12	104.6 (2)
C11–Si–C16	103.9 (2)	MC11–Si–MC12	110.1 (3)
Si–C11–C12	127.7 (3)	Si–C16–C17	125.4 (3)
Si–C11–C15	124.7 (3)	Si–C16–C20	128.2 (3)
MC*n*–C*n*–C (Cp* rings) range: 124.2 (4)–127.5 (4)			
C–C–C (Cp* rings) range: 107.6 (4)–108.3 (4)			
C–C–C (Cp rings) range: 105.0 (4)–110.2 (4)			

[a] Cp**n* denotes the centroid of a permethylcyclopentadienyl ring and Cp*n* denotes the centroid of a cyclopentadienyl ring in the bridging $[SiMe_2(C_5H_4)_2]^{2-}$ ligand. Cp*1, Cp*2, Cp1, and Cp2 contain carbon atoms C1–C5, C6–C10, C11–C15, and C16–C20, respectively. [b] The esd's for the interatomic distances and bond angles were calculated from the standard errors of the fractional coordinates of the corresponding atomic positions. [c] MC denotes a methyl carbon atom.

Table IV. Selected Interatomic Distances (Å) and Bond Angles (deg) for the Non-Hydrogen Atoms in $[SiMe_2(C_5H_4)_2][(C_5H_5)ZrCl]_2(\mu\text{-}O)$[a,b]

A. Interatomic Distances			
Zr1–Cl1	2.480 (1)	Zr2–Cl2	2.460 (1)
Zr1–O	1.944 (2)	Zr2–O	1.944 (2)
Zr1–Cp1	2.221 (4)	Zr2–Cp2	2.234 (4)
Zr1–Cp3	2.221 (4)	Zr2–Cp4	2.232 (4)
Si–C1	1.869 (3)	Si–C6	1.865 (3)
Si–C11	1.853 (4)	Si–C12	1.858 (4)
Zr–C (bridged Cp1 and Cp2 rings) range: 2.507 (3)–2.558 (3)			
Zr–C (Cp3 and Cp4 rings) range: 2.484 (4)–2.530 (4)			
C–C (bridged Cp1 and Cp2 rings) range: 1.375 (5)–1.420 (4)			
C–C (Cp3 and Cp4 rings) range: 1.356 (8)–1.398 (7)			
B. Bond Angles			
Cl1–Zr1–O	96.86 (5)	Cl2–Zr2–O	97.98 (5)
Cp1–Zr1–Cp3	128.4 (2)	Cp2–Zr2–Cp4	127.3 (1)
Zr1–O–Zr2	178.6 (1)		
C1–Si–C11	109.1 (2)	C6–Si–C11	108.0 (2)
C1–Si–Cl2	106.6 (2)	C6–Si–C12	108.5 (1)
Cl-Si–C6	112.1 (1)	C11–Si–C12	112.5 (2)
Si–Cl–C2	129.6 (2)	Si–C6–C7	129.6 (2)
Si–C1–C5	124.8 (2)	Si–C6–C10	125.8 (2)
C–C–C (bridged Cp1 and Cp2 rings) range: 104.5 (2)–110.0 (3)			
C–C–C (Cp3 and Cp4 rings) range: 105.9 (4)–109.1 (5)			

[a] Cp*n* denotes the centroid of a cyclopentadienyl ring. Cp1, Cp2, Cp3, and Cp4 contain carbon atoms C1–C5, C6–C10, C13–C17, and C18–C22, respectively. [b] The esd's for the interatomic distances and bond angles were calculated from the standard errors for the fractional coordinates of the corresponding atomic positions.

of the center of inversion at $^1/_2, {}^1/_2, {}^1/_2$. These peaks were assigned to a highly disordered molecule of toluene. The coordinates for the carbon atoms of the toluene were calculated by fitting the observed peaks to an idealized structure using MIRAGE.[18] These carbon atoms were included as fixed contributions and weighted as half-atoms. Following the inclusion of the toluene of solvation, the remainder of the structure for $[SiMe_2(C_5H_4)_2][(C_5Me_5)ZrCl_2]_2$ refined smoothly. The presence of interstitial toluene was confirmed by measuring the ^1H NMR spectrum of a $CDCl_3$ solution prepared by dissolving crystals of this compound that were grown from toluene. All of the hydrogen atoms were located by difference Fourier methods using only low-angle data with $(\sin\theta)/\lambda < 0.40$ A^{-1}. Full-matrix least-squares refinement (based on F_o^2)[19–23] converged satisfactorily giving the corresponding final discrepancy indices summarized in Table II. A final difference Fourier calculation revealed some residual electron density only in the vicinity of the disordered toluene.

Selected interatomic distances and bond angles for the nonhydrogen atoms in $[SiMe_2(C_5H_4)_2][(C_5Me_5)ZrCl_2]_2$ and [SiMe$_2$-

---

(18) Calabrese, J. C. Ph.D. Dissertation, University of Wisconsin, Madison, WI, 1971; Appendix II.

(19) The least-squares refinement[20] of the X-ray diffraction data was based upon the minimization of $\sum w_i|F_o^2 - S^2F_c^2|^2$, where w_i is the individual weighting factor and S is the scale factor. The discrepancy indices were calculated from the expressions: $R(F_o) = \sum||F_o| - |F_c||/\sum|F_o|$, $R(F_o^2) = \sum|F_o^2 - F_c^2|/\sum F_c^2$, and $R_w(F_o^2) = [\sum w_i|F_o^2 - F_c^2|^2/\sum w_i F_o^4]^{1/2}$. The standard deviation of an observation of unit weight, σ_1, equals $[\sum w_i|F_o^2 - F_c^2|/(n - p)]^{1/2}$, where n is the number of observations and p is the number of parameters varied during the last refinement cycle.

(20) The scattering factors employed in all of the structure factor calculations were those of Cromer and Mann[21] for the non-hydrogen atoms and those of Stewart et al.[22] for the hydrogen atoms with corrections included for anomalous dispersion.[23]

(21) Cromer, D. T.; Mann, J. B. *Acta Crystallogr., Sect. A: Cryst. Phys., Diffr., Theor. Gen. Crystallogr.* **1968**, *A24*, 321.

(22) Stewart, R. F.; Davidson, E. R.; Simpson, W. T. *J. Chem. Phys.* **1965**, *42*, 3175.

(23) Cromer, D. T.; Liberman, D. *J. Chem. Phys.* **1970**, *53*, 1891.

$(C_5H_4)_2][(C_5H_5)ZrCl]_2(\mu\text{-}O)$ are listed in Tables III and IV, respectively. Tables of the final positional and thermal parameters, all of the bond distances and angles, the calculated least-squares planes, and the observed and calculated structure factors are available as supplementary material[24] for these two compounds. The positional and thermal parameters for $[CH_2(C_5H_4)_2][(C_5H_5)ZrCl]_2(\mu\text{-}O)\cdot C_6H_6$ have also been deposited.

Results and Discussion

Synthesis of Binuclear Zirconocenophane Complexes. The metathetical reaction of $Li_2[X(C_5H_4)_2]$ with 2 equiv of $(C_5R_5)ZrCl_3$ provides a convenient method for the preparation of several binuclear zirconocenophane complexes $[X(C_5H_4)_2][(C_5R_5)ZrCl_2]_2$, where (X = CH_2 or $SiMe_2$ and R = H or Me (eq 2). Since this reaction must

$$2(C_5R_5)ZrCl_3 + Li_2[X(C_5H_4)_2] \rightarrow [X(C_5H_4)_2][(C_5R_5)ZrCl_2]_2 + 2LiCl \quad (2)$$

be performed in a stoichiometric manner, it is imperative that the two starting materials be of high quality to optimize yields. Consequently, $(C_5H_5)ZrCl_3$ is converted to the more soluble, crystallizable THF adduct and $(C_5Me_5)ZrCl_3$ is sublimed prior to use. To minimize contamination from chloride ion, the synthesis of $Li_2[SiMe_2(C_5H_4)_2]$ has been modified by extracting $SiMe_2(C_5H_5)_2$ with pentane from the insoluble residue containing NaCl prior to metallation with *n*-butyllithium. This extraction step eliminates the need to distill $SiMe_2(C_5H_5)_2$. On the other hand, the synthesis of $Li_2[CH_2(C_5H_4)_2]$ appears to work best when the $CH_2(C_5H_5)_2$ is distilled under reduced pressure prior to its conversion to the dilithio salt. Hydrolysis of $[X(C_5H_4)_2][(C_5H_5)ZrCl_2]_2$ in the presence of aniline affords a convenient route for preparing the oxo-bridged derivatives $[X(C_5H_4)_2][(C_5H_5)ZrCl]_2(\mu\text{-}O)$ in good yield (eq 3).

$$[X(C_5H_4)_2][(C_5H_5)ZrCl_2]_2 + 2C_6H_5NH_2 + H_2O \rightarrow [X(C_5H_4)_2][(C_5H_5)ZrCl]_2(\mu\text{-}O) + 2C_6H_5NH_3Cl \quad (3)$$

NMR Data. The ^1H and ^{13}C NMR data given in Table I for these binuclear zirconocenophane complexes reveal that the proton and carbon resonances of the bridged bis(cyclopentadienyl) ligand are strongly dependent upon the coordination environment of each Zr(IV) metal center. For $[X(C_5H_4)_2][(C_5R_5)ZrCl_2]_2$, the distal and proximal protons of the $[X(C_5H_4)_2]^{2-}$ ligand exhibit a characteristic pseudo-A_2B_2 splitting pattern with the high-field triplet assigned to the distal protons. In contrast, the presence of the oxo bridge in $[X(C_5H_4)_2][(C_5H_5)ZrCl]_2(\mu\text{-}O)$ introduces a chiral ligand arrangement about each Zr center. As a result, the distal and proximal protons form diastereotopic pairs that produce a more complex ABCD splitting pattern characterized by four distinct multiplets in the aromatic region. The remaining proton resonances for the methyl protons of the dimethylsilyl bridge, the methylene protons of the methylene bridge, and the protons of the free C_5H_5 or C_5Me_5 rings appear as singlets and are readily assignable.

An interesting spectral feature associated with the ^1H NMR spectra of the four $[X(C_5H_4)_2][(C_5R_5)ZrCl_2]_2$ complexes is the chemical shift difference, $\Delta\delta = |\delta_d - \delta_p|$, between the distal ($\delta_d$) and proximal ($\delta_p$) protons. Although our NMR data is limited to a relatively small number of compounds, the value of $\Delta\delta$ appears to be sensitive to the type of free cyclopentadienyl ligand (i.e. C_5H_5 vs C_5Me_5) and the mode of coordination (i.e. bridging vs chelating) for the $[X(C_5H_4)_2]^{2-}$ ligand. Specifically, the magnitude of $\Delta\delta$ observed for $[X(C_5H_4)_2][(C_5H_5)ZrCl_2]_2$ ranges from 0.14 to 0.16 ppm when R = H and from 0.32 to 0.33 ppm when R = Me. However, these values of $\Delta\delta$ are well below the corresponding range of 0.94–1.00 ppm observed for $\Delta\delta$ in several ansa-zirconocene dichloride complexes $[Si(alkyl)_2(C_5H_4)_2]ZrCl_2$, where alkyl = Me, Et, and *n*-Pr.[25] Consequently, when the distal (and proximal) protons remain magnetically equivalent, $\Delta\delta$ may provide an appropriate spectroscopic parameter for distinguishing between the bridging and chelating modes of coordination for a mechanically linked bis(cyclopentadienyl) ligand.

The coordination environment about each Zr is also reflected by the number of ring carbon resonances observed in the ^{13}C NMR spectra for the $[X(C_5H_4)_2]^{2-}$ ligand of these binuclear zirconocenophane compounds. Three distinct resonances corresponding to the bridgehead, distal, and proximal carbons of the bridged cyclopentadienyl rings are found for $[X(C_5H_4)_2][(C_5H_5)ZrCl_2]_2$, whereas five resonances (as expected) are observed for $[X(C_5H_4)_2][(C_5H_5)ZrCl]_2(\mu\text{-}O)$. The bridgehead carbon is readily identified by its low intensity and the lack of $^1J_{C\text{-}H}$ coupling in the corresponding gated nondecoupled ^{13}C NMR spectrum.

The chemical shift of the bridgehead carbon appears to be sensitive to the mode of coordination of the $[X(C_5H_4)_2]^{2-}$ ligand. For these binuclear zirconocenophane complexes (Table I), this carbon resonance is typically found downfield from the proximal and distal carbon resonances. The exact opposite situation for the bridgehead carbon resonance is observed in the ^{13}C NMR spectra of the mononuclear ansa-zirconocene dichlorides $[Si(alkyl)_2(C_5H_4)_2]ZrCl_2$.[25] In addition, although the proximal and distal carbon resonances of the $[SiMe_2(C_5H_4)_2]^{2-}$ ligand are fairly insensitive to its mode of coordination, the bridgehead carbon resonance of $[SiMe_2(C_5H_4)_2][(C_5R_5)ZrCl_2]_2$ is found 15–20 ppm downfield from that of $[SiMe_2(C_5H_4)_2]ZrCl_2$.

The chemical shift of the bridgehead carbon is further influenced by the type of bridging group, X, of the $[X(C_5H_4)_2]^{2-}$ ligand. Specifically, a larger downfield shift is observed for X = CH_2 than X = $SiMe_2$. This result presumably reflects an alteration in the π-electron density at the bridgehead carbon. Replacement of $SiMe_2$ with the shorter CH_2 bridge enhances the repulsion between the π-electron clouds of the two aromatic rings. Qualitatively, this interaction should shift more of the π-electron density away from the bridgehead carbon, thereby leading to a larger downfield shift of its carbon resonance.

Description of the Molecular Structures of $[SiMe_2(C_5H_4)_2][(C_5Me_5)ZrCl_2]_2$ and $[SiMe_2(C_5H_4)_2][(C_5H_5)ZrCl]_2(\mu\text{-}O)$. The molecular structures of $[SiMe_2(C_5H_4)_2][(C_5Me_5)ZrCl_2]_2$ and $[SiMe_2(C_5H_4)_2][(C_5H_5)ZrCl]_2(\mu\text{-}O)$ have been determined by X-ray diffraction methods. The former compound crystallizes in the triclinic space group $P\bar{1}$ with one molecule of toluene disordered about a center of inversion in each unit cell. The oxo-bridged compound crystallizes in the monoclinic space group $P2_1/c$ with four discrete molecules per unit cell. The solid-state structures of both binuclear zirconocenophane complexes are well-behaved, and perspective views of their molecular configurations are depicted in Figures 1 and 2, respectively, with appropriate atom numbering schemes.

In both compounds the $[SiMe_2(C_5H_4)_2]^{2-}$ acts as a bridging ligand linking two $(C_5R_5)ZrL_2$ units. The coordination environment about each Zr(IV) center is analogous to the pseudotetrahedral ligand arrangement reported

---

(24) The computer programs employed during the X-ray structural analyses are described in Nicholson, G. A.; Petersen, J. L.; McCormick, B. J. *Inorg. Chem.* **1980**, *19*, 195.

(25) Bajgur, C. S.; Tikkanen, W. R.; Petersen, J. L. *Inorg. Chem.* **1985**, *24*, 2539.

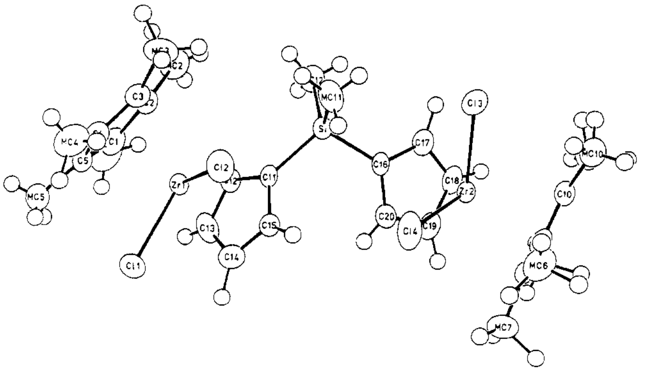

Figure 1. Perspective view of the molecular configuration of $[SiMe_2(C_5H_4)_2][(C_5Me_5)ZrCl_2]_2$ with the atom-labeling scheme for the non-hydrogen atoms. The thermal ellipsoids are scaled to enclose 50% probability. For clarity the radii of the spheres for the hydrogen atoms were reduced arbitrarily.

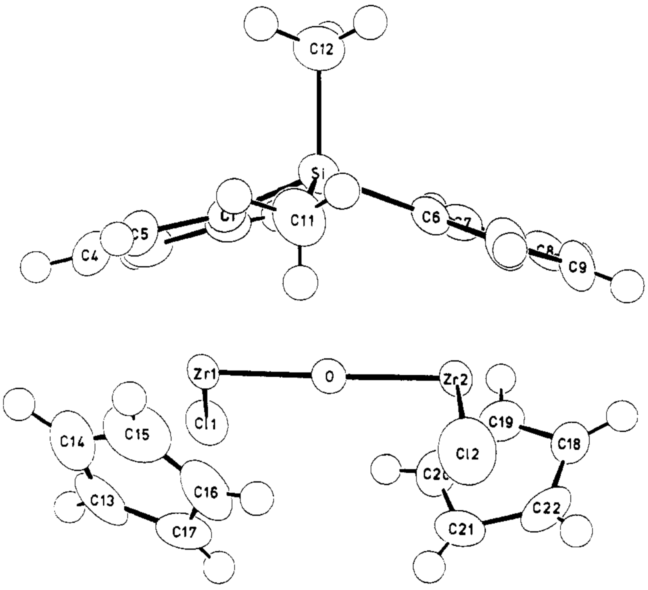

Figure 2. Perspective view of the molecular configuration of $[SiMe_2(C_5H_4)_2][(C_5H_5)ZrCl]_2(\mu\text{-}O)$ with the atom-labeling scheme for the non-hydrogen atoms.

for numerous Cp_2ZrL_2-type complexes.[26] The ring centroid–Zr–ring centroid and L–Zr–L angles fall within the expected ranges of 125–135° and 95–100°, respectively.

Due to the steric bulk of the permethylated cyclopentadienyl rings in $[SiMe_2(C_5H_4)_2][(C_5Me_5)ZrCl_2]_2$, the cyclopentadienyl rings of the bridging $[SiMe_2(C_5H_4)_2]^{2-}$ ligand are rotated about the Si–C(bridgehead) bonds, thereby producing a molecular geometry characterized by a long Zr1···Zr2 separation of 7.260 (1) Å. The magnitude of this rotation can be estimated from the dihedral angle, θ, between the corresponding lines passing through each pair of proximal carbons of the linked five-membered rings. In the absence of rotation, the angle θ made by these two lines when projected on a two-dimensional plane should be zero. This symmetrical arrangement of the C_5H_4 rings is observed for the chelating $[SiMe_2(C_5H_4)_2]^{2-}$ ligand in $[SiMe_2(C_5H_4)_2]ZrCl_2$.[25] By comparison, the corresponding value of θ in $[SiMe_2(C_5H_4)_2][(C_5Me_5)ZrCl_2]_2$ is 47.5°. In addition, as evident from the perspective view illustrated in Figure 1, both $(C_5Me_5)ZrCl_2$ fragments are positioned on the respective C_5H_4 faces of the bridging ligand so that any potential inter-ring repulsions arising from rotations about the two Si–C bonds are minimized in solution.

Table V. Available Structural Data for Related Oxo-Bridged Zirconium Dimers

ref	compound	ϕ,[a] deg	Zr–O, Å	Zr–O–Zr, deg	L–Zr–O,[b] deg
29	$[Cp_2ZrCl]_2O$	74.3	1.94 (1)	168.9 (8)	99.3 (4)
			1.95 (1)		96.8 (5)
30	$[Cp_2Zr(SC_6H_5)]_2O$	61.7	1.968 (3)	165.8 (2)	98.7 (1)
			1.964 (3)		103.3 (1)
26c	$[Cp_2Zr(CH_3)]_2O$		1.948 (1)	174.1 (3)	96.3 (2)
this work	$[SiMe_2(C_5H_4)_2]$-$[CpZrCl]_2O$	45.4	1.944 (2)	178.6 (1)	96.86 (5)
			1.944 (2)		97.98 (5)
31	$[CH_2(C_5H_4)_2]$-$[CpZrCl]_2O$	47.7	1.938 (5)	174.3 (2)	98.8 (1)
			1.938 (4)		97.6 (2)
8q	$(C_{10}H_8)[CpZrCl]_2O$		1.943 (1)	156.0 (2)	98.1 (1)

[a] ϕ is the dihedral angle between the two L–Zr–O planes. [b] L represents the monodentate ligand (CH_3, SC_6H_5, Cl) bonded to the metal atom in these oxo-bridged dimers.

Replacement of each C_5Me_5 group by the smaller C_5H_5 ligand should permit a closer approach of the Zr(IV) centers. This remark is borne out by the fact that hydrolysis of $[SiMe_2(C_5H_4)_2][(C_5H_5)ZrCl_2]_2$ introduces an intramolecular oxo bridge that links the two zirconium atoms together. The Zr1···Zr2 separation in $[SiMe_2(C_5H_4)_2][(C_5H_5)ZrCl]_2(\mu\text{-}O)$ is now 3.89 (1) Å. The oxo bridge also produces a more symmetrical disposition of the bridged cyclopentadienyl rings, as reflected by a dihedral angle, θ, of 4.2°.

The oxo bridge further influences several other structural parameters associated with these binuclear zirconocenophanes. In general, as shown in Table V, the Zr–O bonds in binuclear oxo-bridged zirconocene complexes are ca. 0.2 Å shorter than a normal Zr–O single bond of 2.15–2.20 Å.[27] This reduction in the Zr–O distances reflects a significant amount of multiple-bond character, arising from π-donation from the filled p_π orbitals of the oxo ligand to the corresponding empty dz^2-like LUMO of each Zr(IV) center.[28] This bonding interaction reduces the electrophilicity of each electron-deficient metal, leading to a small but consistent increase of 0.03–0.04 Å in the Zr–Cl and Zr–ring centroid distances. For example, the average Zr···Cp(centroid) and Zr–Cl bond distances in $[SiMe_2(C_5H_4)_2][(C_5H_5)ZrCl]_2(\mu\text{-}O)$ are 2.225 and 2.470 Å, respectively, whereas their averaged values in $(C_5H_5)_2ZrCl_2$[26a] are 2.195 and 2.440 Å, respectively.

To optimize the π-donation from the two orthogonal O p_π orbitals, the oxo-bridged zirconocene dimers $[(C_5H_5)_2ZrL]_2(\mu\text{-}O)$ (L = Cl,[29] SC_6H_5,[30] or CH_3[26c]) should adopt a molecular geometry with the dihedral angle between the two L–Zr–O planes being near 90° and characterized by a linear Zr–O–Zr bridge.[28,30] However, as noted in Table V, these angles differ significantly from these ideal values. In the corresponding mechanically linked zirconocenophane complexes, the orientation of the O–Zr–Cl planes is strongly influenced by the bridging bis(cyclopentadienyl) ligand since it constrains the relative orientation of each Zr acceptor orbital with respect to the pair of O p_π donor orbitals. As a result, the optimal di-

---

(26) (a) Prout, K.; Cameron, T. S.; Forder, R. A.; Critchley, S. R.; Denton, B.; Rees, G. V. *Acta Crystallogr., Sect. B* **1974**, *B30*, 2290. (b) Jeffrey, J.; Lappert, M. F.; Luong-Thi, N. T.; Webb, M.; Atwood, J. L.; Hunter, W. E. *J. Chem. Soc., Dalton Trans.* **1981**, 1953 and references cited therein. (c) Hunter, W. E.; Hrncir, D. C.; Bynum, R. V.; Pentilla, R. A.; Atwood, J. L. *Organometallics* **1983**, *2*, 750.

(27) Silver, M. E.; Chun, H. Y.; Fay, R. C. *Inorg. Chem.* **1982**, *21*, 3765 and references cited therein.

(28) Lauher, J. W.; Hoffmann, R. *J. Am. Chem. Soc.* **1976**, *98*, 1729 and references cited therein.

(29) Clarke, J. F.; Drew, M. G. B. *Acta Crystallogr., Sect. B* **1974**, *B30*, 2267.

(30) Petersen, J. L. *J. Organomet. Chem.* **1979**, *166*, 179.

hedral angle between the O–Zr–Cl planes of $[X(C_5H_4)_2][(C_5H_5)ZrCl]_2(\mu\text{-}O)$ is more or less set at ca. 45°. Further, the distance between the ring centroids of the bridged cyclopentadienyl rings affects the Zr–O–Zr bond angle by altering the directional properties of the acceptor orbitals involved in oxo-bridge formation. A decrease in this distance from 4.95 (1) Å in $[SiMe_2(C_5H_4)_2][(C_5H_5)ZrCl]_2(\mu\text{-}O)$ to 4.82 (1) Å[31] in $[CH_2(C_5H_4)_2][(C_5H_5)ZrCl]_2(\mu\text{-}O)$ to 3.84 Å (estimated) in $(C_{10}H_8)[(C_5H_5)ZrCl]_2(\mu\text{-}O)$[8q] is accompanied by a parallel reduction in the Zr–O–Zr bond angle from 178.6 (2)° to 174.3 (2)° to 156.0 (2)°, respectively. Consequently, the size/length of the bridging linkage exhibits a significant influence on the central geometry of these modified oxo-bridged zirconocene complexes.

In summary, convenient synthetic procedures have been developed for the preparation of a new class of binuclear zirconocenophane complexes. The availability of $[X(C_5H_4)_2][(C_5R_5)ZrCl_2]_2$ and $[X(C_5H_4)_2][(C_5H_5)ZrCl]_2(\mu\text{-}O)$ has provided appropriate starting materials for synthesizing other binuclear derivatives, including $[SiMe_2(C_5H_4)_2][(C_5H_5)ZrL(\mu\text{-}H)]_2$ (L = H, Cl) and $[SiMe_2(C_5H_4)_2][(C_5H_5)Zr(\mu\text{-}Cl)]_2$.[32] Current efforts are directed at exploring the potential cooperative chemical effects introduced by the near proximity of two high-valent zirconium centers in these zirconocenophane complexes.

Acknowledgment. Support for this research was provided by the West Virginia Energy and Water Research Center. Computer time for the X-ray structural analyses was provided by the West Virginia Network for Educational Telecomputing.

Registry No. CH_2Br_2, 74-95-3; $SiMe_2Cl_2$, 75-78-5; $CH_2(C_5H_5)_2$, 79249-50-6; $SiMe_2(C_5H_5)_2$, 18053-74-2; $Li_2[CH_2(C_5H_4)_2]$, 121706-37-4; $Li_2[SiMe_2(C_5H_4)_2]$, 87122-68-7; $(C_5H_5)ZrCl_3$, 34767-44-7; $(C_5Me_5)ZrCl_3$, 75181-07-6; $[SiMe_2(C_5H_4)_2][(C_5Me_5)ZrCl_2]_2$, 121730-60-7; $[SiMe_2(C_5H_4)_2][(C_5H_5)ZrCl_2]_2$, 118920-56-2; $[CH_2(C_5H_4)_2][(C_5Me_5)ZrCl_2]_2$, 121730-61-8; $[CH_2(C_5H_4)_2][(C_5H_5)ZrCl_2]_2$, 121730-62-9; $[SiMe_2(C_5H_4)_2[(C_5H_5)ZrCl]_2(\mu\text{-}O)$, 118920-57-3; $[CH_2(C_5H_4)_2][(C_5H_5)ZrCl]_2(\mu\text{-}O)$, 121730-63-0; $[SiMe_2(C_5H_4)_2][(C_5Me_5)ZrCl_2]_2\cdot{}^1/_2C_7H_8$, 121754-77-6; $[CH_2(C_5H_4)_2][(C_5H_5)ZrCl]_2(\mu\text{-}O)\cdot C_6H_6$, 121730-64-1.

Supplementary Material Available: Tables of positional and thermal parameters, interatomic distances and bond angles, and least-squares planes for the X-ray structural analyses of $[SiMe_2(C_5H_4)_2][(C_5Me_5)ZrCl_2]_2\cdot{}^1/_2C_7H_8$ and $[SiMe_2(C_5H_4)_2][(C_5H_5)ZrCl]_2(\mu\text{-}O)$ and a table of the refined positional and thermal parameters for the X-ray structure determination of $[CH_2(C_5H_4)_2][(C_5H_5)ZrCl]_2(\mu\text{-}O)\cdot C_6H_6$ (31 pages); listings of observed and calculated structure factors (34 pages). Ordering information is given on any current masthead page.

---

(31) Crystal data for $[CH_2(C_5H_4)_2][(C_5H_5)ZrCl]_2(\mu\text{-}O)\cdot C_6H_6$: space group $P\bar{1}$, $a = 11.891$ (4) Å, $b = 12.736$ (5) Å, $c = 13.129$ (6) Å, $\alpha = 114.02$ (3)°, $\beta = 115.34$ (2)°, $\gamma = 111.39$ (3)°, $V = 1243.6$ (7) Å^3, $Z = 2$, $d_{calcd} = 1.655$ g/cm^3. Full-matrix refinement (based on F_o^2) with anisotropic temperature factors for the 32 non-hydrogen and isotropic temperature factors for the 26 hydrogen atoms converged with discrepancy indices of $R(F_o) = 0.043$, $R(F_o^2) = 0.045$ and $R_w(F_o^2) = 0.075$ with $\sigma_1 = 1.57$ for 2914 data with $F_o^2 > \sigma(F_o^2)$. A table of refined positional and thermal parameters is included with the supplementary material.

(32) Reddy, K. P.; Petersen, J. L. *Organometallics* **1989**, *8*, 547.

Distinction among Three Possible Radical Chain Mechanisms in the Disproportionation Reactions of $Cp_2Fe_2(CO)_4$ ($Cp = \eta^5\text{-}C_5H_5$)

Michael P. Castellani and David R. Tyler*

Department of Chemistry, University of Oregon, Eugene, Oregon 97403

Received December 22, 1988

The kinetics of the thermal disproportionation reaction of the $Cp_2Fe_2(CO)_4$ complex with dppe (1,2-bis(diphenylphosphino)ethane) were studied so as to differentiate between three possible radical chain mechanisms. The disproportionation reaction is initiated by spontaneous homolysis of the Fe–Fe bond at room temperature in CH_2Cl_2 ($k \approx 2.7 \times 10^{-7}$ s^{-1}). The rate law for the disproportionation reaction is rate = $k[\text{dppe}]^{1/2}[Cp_2Fe_2(CO)_4]$, where $k = 7.0 \times 10^{-4}$ M$^{-1/2}$ s^{-1} at 23 °C in CH_2Cl_2. This rate law is consistent with the radical chain pathway in Scheme I (in which ligand association to a 17-electron $CpFe(CO)_2$ radical is followed by electron transfer and then a fragmentation step) but not with the pathways in Schemes II and III (which involve variations in the sequence of the association, electron transfer, and fragmentation steps). The thermal disproportionation reaction of $Cp_2Fe_2(CO)_4$ with dppe is inhibited by trace impurities in the reaction solution; the reaction could be initiated, however, by brief irradiation of the reaction solution. Presumably, the impurities are removed by reaction with the intermediates formed in the photoreaction. Analysis of the kinetics data by the numerical integration program GIT yielded values for the unknown rate constants in the disproportionation mechanism, including the values for the equilibrium constant for the reaction of $CpFe(CO)_2$ with dppe to form the 19-electron $CpFe(CO)_2(\text{dppe-}P)$ complex ($K_{eq} = 0.91$) and for the termination step in which $CpFe(CO)_2$ reacts with $CpFe(CO)\text{dppe}$ ($k = 7.8 \times 10^7$ M^{-1} s^{-1}). The kinetic chain length for the reaction was calculated to be 460.

Introduction

In a series of papers, we reported the results of our mechanistic studies of the photochemical disproportionation reactions of the $Cp_2Fe_2(CO)_4$,[1] $Cp_2Mo_2(CO)_6$,[2] and $Mn_2(CO)_{10}$[3] complexes (eq 1, shown for the case of

$$Cp_2Fe_2(CO)_4 + L \xrightarrow{h\nu} CpFe(CO)_2L^+ + CpFe(CO)_2^- \quad (1)$$

$$L = PR_3,\ P(OR)_3$$

$Cp_2Fe_2(CO)_4$;[4] analogous reactions occur with the other dimers). The reactions follow a chain pathway, and the